IABSE-JSCE Joint Conference on Advances in Bridge Engineering-IV, August 26-27, 2020, Dhaka, Bangladesh
Amin, Okui, Bhuiyan, Rahman (eds.)

ISBN: 978-984-34-8313-3
www.iabse-bd.org

Field test load rating procedure for skewed highway bridges using grillage modeling

R. Lu & M. Barker
University of Wyoming, Laramie, Wyoming, United States of America

J. Judd
Brigham Young University, Provo, Utah, United States of America

ABSTRACT: An experimental load rating procedure is presented that considers the effect of skew. In the proposed procedure, the bridge is represented using grillage modeling and then tested *in-situ* using a calibrated truck load. The experimentally calculated internal forces and results obtained using grillage modeling are used to determine the experimental live load effect, to evaluate different contributions of the experimental rating capacity, and to compare the analytical live load effects. To illustrate the proposed procedure, a skewed four-span concrete slab on steel girder highway bridge was examined for positive moment. Results indicated a 27% increase in the load rating, even when the effect of unintended composite action is removed. The effect of skew contributes to a 19% increase in the load rating. Considering partial restraint of the abutments, the effect of curbs and railings contributes to an estimated 10% increase in the load rating.

1 INTRODUCTION

It is of utmost importance for engineers to understand the actual behavior of highway bridges to provide necessary protection for the traveling public. However, in conventional practice, bridges are still designed using idealized models and evaluated based on simple visual inspections, often without any site-specific data. As a consequence, the predicted response generally does not correspond to the actual behavior (e.g. Chajes et al. 2000). For instance, the actual longitudinal live load distribution may be different than the analytically determined distribution, and this may lead to incorrect predictions of the load path (e.g. Jáuregui& Barr 2004).Likewise, the effect of skew on the lateral live load distribution and on the stiffness of the structure is not fully accounted for in conventional design (Badwin and Liang 2007). Moreover, in the case of bridges built to behave non-compositely, additional composite action between girders and slab are observed (Yarnold et al. 2018). Even though improvements were made in the AASHTO LRFD (Load and Resistance Factor Design) specifications relative to the AASHTO LFD (Load Factor Design) specifications, the estimations obtained using the AASHTO LRFD are still conservative since they are based on theoretical modeling (Huang et al. 2004). The discrepancies between the analytical and actual behavior can lead to inappropriate postings, re-routings and repairing which cause inconveniences to users and unnecessary budgeting of resources from the departments of transportation (Sanayei et al. 2016). As a result, it is critical to close the gap between the analytical and actual behavior of highway bridges. As a possible solution, the objective of this study is to develop a load rating procedure that employs experimental field testing and grillage modeling. The procedure consists of comparing the contributions to the load capacity due to live load between experimental and analytical results. To demonstrate the procedure, the critical positive moment location of a skewed four-span concrete slab on steel girders Highway Bridge was load rated. Although the focus of this study is on bridges with steel girders and concrete slab, the proposed approach could also be adapted to other types of highway bridge systems.

2 CASE STUDY

2.1 *Methodology*

In the proposed method, the bridge critical moment locations are identified, the experimental and analytical strength inventory rating factors are calculated and used to obtain the bridge ratio of load ratings. Selected

bridge girders are instrumented with strain gages at the maximum positive and near negative moment locations, and a calibrated test truck traverses the bridge in successive lateral runs to capture the response of every girder. The resultant strain-history profile of each girder in the span of interest are recorded for each run and used to calculate peak internal moment and axial forces, separating the non-composite and composite action components. The calculated internal moments obtained for individual truck runs are then superimposed to obtain internal moments for side-by-side truck loadings, which are used to determine the experimental live load effect. The experimental live load is discretized for purposes of comparing rating factors. To determine the analytical live load effect, grillage modeling of an equivalent bridge without skew (a straight bridge) is conducted. Loads corresponding to the critical side-by-side truck loadings are placed at the grillage model to maximize the positive moment, such that the summation of girder moments at the positive, negative, and corresponding statical moment of the system are obtained. Both experimental and analytical live load ratings are calibrated to a standardized design truck whose effect is obtained using the grillage modeling. By taking the ratio between the rating factors, the sources of contribution (including the effects of longitudinal and lateral distributions, additional stiffness in the system, slab flexure and unintended composite action) that increase or decrease the bridge actual capacity in comparison to the analytical estimations are qualified and quantified. To further deaggregate the contributions, the additional stiffness in the structure is separated into contributions due to the bridge skew and due to curbs and railings. The contribution due to the bridge skew is determined by comparing the statical moments between the skewed and non-skewed bridge models.

2.2 *Evanston Bridge Description*

The eastbound highway bridge utilized for the case study is located along Interstate Highway 80 (I-80) in Evanston, Wyoming, and crosses over the Bear River. The bridge (Figure 1) consists of four spans: the outer spans are 25.6-m (84-ft) long and the inner spans are 36.6-m (120-ft) long. It has an angle of skew equal to 43° relative to the abutments and a straight vertical alignment. The girders of the bridge are an I-section shape and are haunched at the interior supports. The bridge was originally constructed with four non-composite girders but was later widened by adding a southern exterior girder designed to behave compositely. To facilitate the nomenclature throughout the paper, as shown in Figure 2, girders were numbered from left to right, relative to the direction of travel (i.e. Girder 1 is the innermost exterior girder and Girder 5 is the outermost exterior girder). The dimension of the concrete slab and clear roadway width is also illustrated in the Figure 2.

Figure 1. Skewed four-span concrete slab on steel girders highway bridge along I-80 in Evanston, Wyoming.
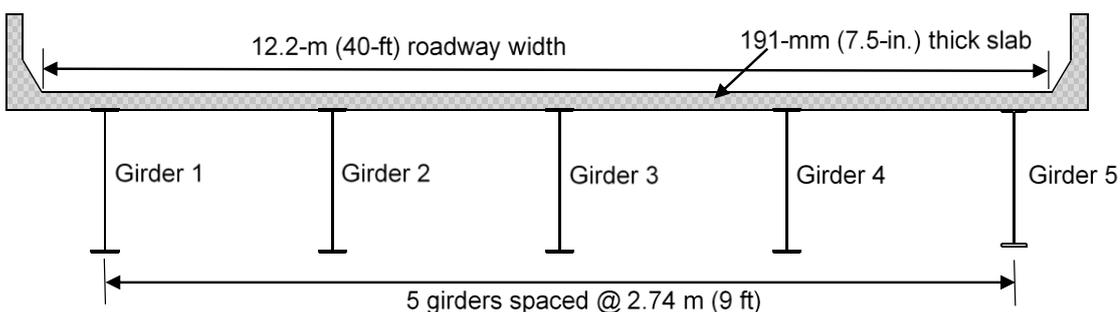

Figure 2. Typical cross-section of the highway bridge.

2.3 *Instrumentation and Field Test*

According to analysis conducted using a one-dimensional girder model, it was verified that the maximum positive moment occurs at the middle of the inner span and the negative moment occurs at the outer pier. However, due to the presence of the Bear River and a railroad which made the installation of the inner span impractical, it was decided to instrument the second most critical location instead, which is located in the eastern outer span at the 0.4 times of the outer span location measured from the abutment.

All five girders in the eastern outer span were instrumented with ST350 strain gages (BDI 2012) at the maximum positive moment and 2.44-m (8-ft) offset from the negative moment (Figure 3). The purpose of the offset given to the strain gages mounted at the negative moment is to avoid interferences with bearings and diaphragms of the pier (Barker 1999). As a rule of thumb, a distance equal to the depth of the girder web was considered. Since the girder depth is 2210 mm (87 in.), a rounded-up value of 2.44 m (8 ft) was chosen. A larger offset value was avoided so that errors of extrapolation (from the instrumented location to the pier) carried out during the analysis are minimized. Since a linear elastic response is expected, two strain gages were installed on each girder and location to obtain the corresponding linear strain profiles. One strain gage was placed at the center of the bottom flange, and the other was placed on the web 102 mm (4 in.) below the bottom of top flange (Figure 4).

Figure 3. Instrumentation of the steel girders at the positive and negative moment locations.
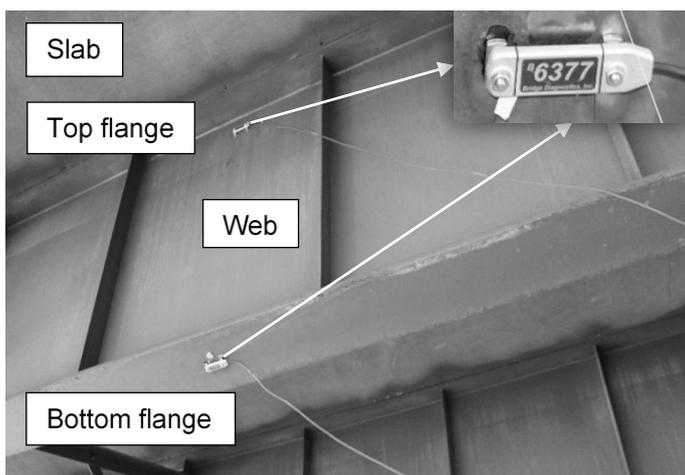

Figure 4. Strain gage placement used to determine the strain profile of the steel girder.

In the field test, a total of fifteen runs across the bridge were conducted using a calibrated truck driven in crawl speed (Figure 5). The total number of runs is that needed to traverse the entire width of the roadway. It was decided to conduct the test from left to right relative to the direction of travel. As required by *The Manual for Bridge Evaluation* (AASHTO 2011), the left wheel of the truck for Run 1 was placed 0.91 m (3 ft) offset from the left curbs (a minimum of 0.61 m (2 ft) is stipulated), and the position of each successive run was offset 0.61 m (2 ft) to the right of the previous run. The gross vehicle weight of the truck used in the field test is

203 kN (45.7 k) in which the front axle and each rear axle weight are 51.2 kN (11.5 k) and 76.1 kN (17.1 k), respectively. The axle spacing is 4.21 m (13.8 ft) between the front and middle axle and 1.31 m (4.3 ft) between the middle and rear axle. The weight of the truck was calibrated so that the bridge response due to the live load still falls within the linear elastic region (Cai & Shahawy 2003).
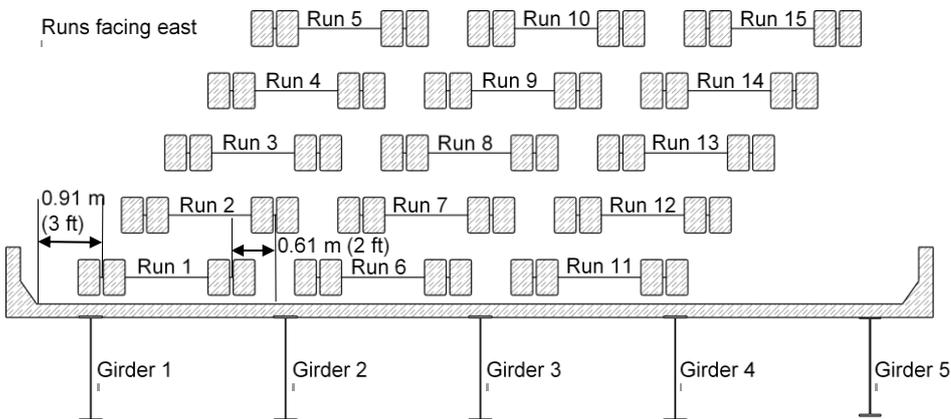

Figure 5. Position of the calibrated truck runs during the field test.

2.4 *Calculation of Internal Forces*

Separate and unique strain-histories were collected in each strain gage and run. For each run, the girder with the peak positive strain and the corresponding time of occurrence were selected. This girder was identified as the critical girder for the run. The time that the peak positive strain occurred was also applied to the other strain gage of the critical girder so that a linear strain profile was obtained. The same selected time was also applied to all the non-critical girders to obtain their respective strain profiles.

Internal stresses were calculated based on the internal strains using the material and geometric properties of the girder and the slab. The total stress profile for each girder was decomposed into an axial component and a flexural component. The girder axial stress, σ_{cg} obtained as the total stress at the girder center of gravity. The maximum girder flexural stress was determined by subtracting the stress at the extreme fiber of the bottom flange, σ_0 to σ_{cg}. The axial force in the girder, N was determined as the product of σ_{cg} and the area of the girder, A_{girder}. The axial force in the slab was assumed to be equal to the axial force in the girder based on equilibrium and no external force. The internal moment in the girder about its own axis, M_{girder} was calculated as the product of the girder flexural stress and the girder section modulus, S_{girder}. The internal moment in the slab about its own axis, M_{slab} was computed as the product of M_{girder} times the ratio of the slab flexural stiffness, $(EI)_{slab}$ and the girder flexural stiffness, $(EI)_{girder}$. The internal moment due to interaction between girder and slab was calculated as the product of N times the distance from the center of gravity of the girder to the center of gravity of the slab, a. The total internal moment for a girder, M_{total} was then the sum of the internal moments. The decomposition of the different components is illustrated in Figure 6.
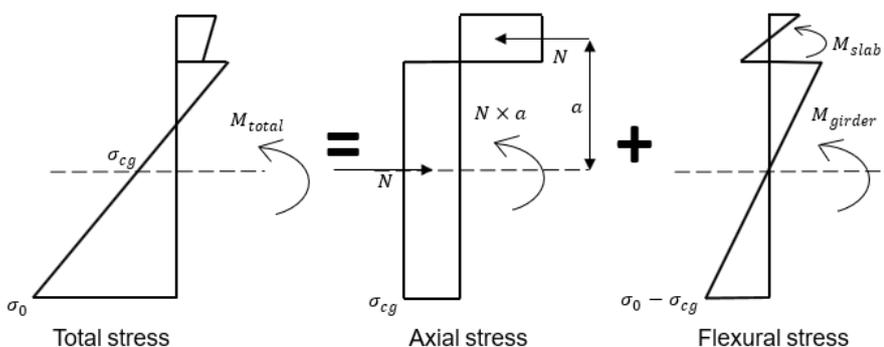

Figure 6. Decomposition of the calculated internal stress profile

It was expected that side-by-side truck loading would control (i.e. produce larger internal moments) compared to a single truck load even though the former was subjected to a reduction to account the improbability of

coincident maximum loading. Therefore, the computation of internal moments shown in Figure 6 was repeated for every girder of each run and superimposed to obtain the internal moments for side-by-side truck loadings. In addition, the superposition was also applied for the computation of statical moments required later. For the side-by-side truck loadings, the critical girder is the girder subjected to the maximum value of the summation of peak strains. The results showed that the side-by-side truck loading involving Runs 3, 8 and 13 superimposed controlled at the positive moment location with the maximum total moment occurring in Girder 3. The three side-by-side truck loading controlled even though only 90% of the live load was used to account for the improbability of coincident maximum loading, as defined in *Standard Specifications for Highway Bridges* (AASHTO 1996). This is equivalent to a multiple presence factor for live load, m equal to 0.9 (*LRFD Bridge Design Specifications* (AASHTO 2015)). For single and two side-by-side truck loadings, m is equal to 1.0. The values of M_{girder}, M_{slab}, $N \times a$ and M_{total} for the critical side-by-side truck loading are equal to 317 kN-m (234 k-ft), 5.24 kN-m (3.87 k-ft), 239 kN-m (176 k-ft), 561 kN-m (414 k-ft), respectively. In addition, the summation of the positive and negative moments in all girders are equal to 1800 kN-m (1330 k-ft) and -575 kN-m (-424 k-ft), respectively which yield an experimental statical moment, $\sum STAT_E$ equal to 2210 kN-m (1630 k-ft).

2.5 *Grillage Modeling*

For the theoretical modeling, a non-skewed (straight) grillage model of the bridge was produced using SAP2000 (CSI 2000). The skew angle was not considered because otherwise, the contribution due to the bridge skew on load rating would not be able to quantify. To obtain this effect, a skewed bridge model was produced after, whose statical moment was compared with the statical moment of the original model.

The mesh of the grillage models was assembled with five longitudinal girders and five main transverse elements with the respective fixity that represent the abutments and piers. The transverse mesh has a spacing of 2.74 m (9 ft), which corresponds to the transverse spacing between girders, and the standard longitudinal mesh has a spacing of 1.28 m (4.19 ft). The longitudinal spacing was not always followed since nodes were inserted to demarcate locations with punctual transverse elements such as cross-frames and locations where there is a change in the sectional properties. All longitudinal and transverse elements were modeled using "Frame" elements provided by the software and assigned with material and geometric properties. For purposes of calculating the analytical moments, all the elements were modeled to act fully composite since it assimilates to the actual bridge behavior. Even though Girders 1 through 4 were design to act non-compositely, composite action was verified since the friction between girders and slab is not overcome for live load responses that still fall within the linear elastic region (Lantsoght et al. 2017). A generic section was assigned to each element with the attribution of respective moment of inertia relative to the strong axis and torsional constant (the predominant parameters). The shear area was not considered and therefore no shear deformation was included in the analysis All the elements were assigned with the material properties of an A36 steel. To model the elements of concrete, the material was assumed to be uncracked, and the compressive strength is equal to 22.4-MPa (3.25 ksi) and 27.6-MPa (4 ksi) for the original and new added girders, respectively. In the composite elements, the concrete contribution was transformed into steel based on the respective modular ratio. At the haunched portion of the bridge, the elements were discretized so that the values of composite moment of inertia and torsional constant were equal to the average value of what would be obtained at the start and end nodes of each element. The bridge curbs were modeled by combining them with the exterior girders. The width of the curbs was added to the originally assumed tributary width so that the moment of inertia and torsional constant were added to the original composite girder-slab system. A 3D view of the grillage model is illustrated in Figure 7.

To model the loading, each truck was represented using concentrated loads which correspond to the respective wheel loads of the truck. Loads corresponding to the critical side-by-side truck loading (Runs 3, 8 and 13) were placed on the grillage. To maximize the positive moment, the loads corresponding to the middle axles of each truck were placed at a distance 0.4 times the span length measured from the abutment of the eastern span. For the locations of interest, it was observed that none of the concentrated loads fell exactly on the grillage nodes. Therefore, the loads were distributed to the corners of unit mesh (that envelopes the original load) based on an inverse relationship relative to the respective distance.

For the computation of both analytical and experimental live load effects, the analytical moment due to a standardized truck is required. In this study, it was opted to follow the specifications of the LFD (Load Factor Design) approach given in the *Standard Specifications for Highway Bridges* which stipulates the use of a standardized HS20 design truck. Since the bridge was originally constructed using this approach, it makes the comparison with the existing results easier. The loads corresponding to three standardized HS20 design trucks were modeled and placed at the same position that corresponds to the critical side-by-side truck loading with

the middle of the respective trucks at a distance 0.4 times the span length measured from the abutment of the eastern span.
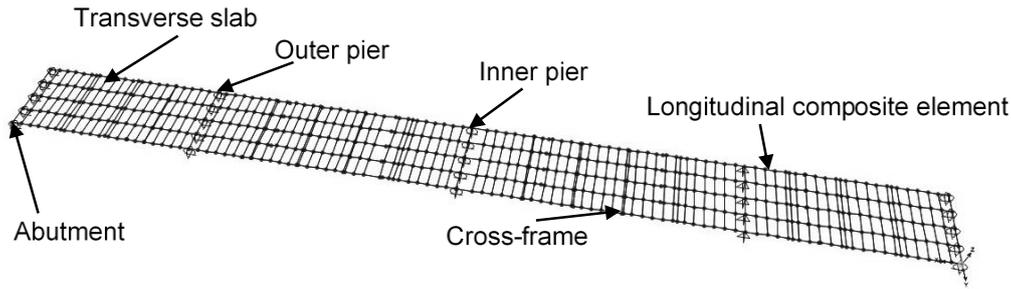

Figure 7. Three-dimensional view of the equivalent straight bridge grillage model.

A linear static load case was defined before running the model. The effect of the self-weight was removed so that only the responses due to the assigned loads are analyzed. Since the live load was calibrated so that the effect falls within the linear elastic region, geometric and material nonlinearities were not considered. With the completion of the analysis, the moments at the maximum positive and negative moment locations for each girder were recorded. For the critical side-by-side truck loading due to the calibrate trucks, the sum of the moments of each girder at positive and negative moment locations were obtained as well as the corresponding statical moment. The positive and negative moments are equal to 2880 kN-m (2120 k-ft) and -885 kN-m (-653 k-ft), respectively, and the statical moment, $\sum STAT_{A,ST}$ is equal to 3230 kN-m (2380 k-ft). Also, the positive moment obtained at Girder 3, $3M_{TRK,max,girder}$ is equal to (709 kN-m) 523 k-ft. For the side-by-side truck loading due to the standardized HS20 design trucks, only the positive moment obtained at Girder 3, $3M_{HS20,max,girder}$ is required, and it takes a value of 1040 kN-m (764 k-ft).

   To obtain the contribution of the bridge skew in the additional stiffness, a skewed bridge model with identical properties were made, and its statical moments was compared with the value obtained in the straight bridge model. The modeling and load application are identical to the methods applied for the straight bridge model. To determine the maximum positive moment, the position was assumed to be relative to the 0.4 times the span length measured from the abutment of the eastern span of Girder 3. As a result, the total positive and negative moments of this model are equal to 2410 kN-m (1780 k-ft) and -750 kN-m (-553 k-ft), respectively, and the statical moment, $\sum STAT_{A,SK}$ is equal to 2710 kN-m (2000 k-ft).

3 RESULTS

3.1 *Live Load Effects and Rating Factors*

To calculate the experimental and analytical live load effects, LL_E and LL_A, respectively, the internal moment in the girder was scaled to the standardized HS20 design truck load and is obtained as the following:

$$LL_E = \left(\frac{3M_{HS20,max,girder}}{3M_{TRK,max,girder}}\right) M_{girder}\, m \qquad (1)$$

$$LL_A = 3M_{HS20,max,girder}\, m \qquad (2)$$

   As a result, LL_E is equal to 418 kN-m (308 k-ft), and LL_A is equal to 934 kN-m (688 k-ft). According to the *Standard Specifications for Highway Bridges*, the strength inventory rating factor, $RF_{strength\_inventory}$ is calculated as follows:

$$RF_{strength\_inventory} = \frac{R_n - 1.3D}{2.17LL(1+I)} \qquad (3)$$

where R_n is the capacity of the member, D is the dead load effect of the member, LL is the live load effect of the member and I is the dynamic impact factor. Since no field inspections were carried out, the nominal dimensions of the members were assumed for the calculations of both experimental and analytical R_n and D. R_n is obtained as the product of the yield strength of the girder to S_{girder} (properties of the critical girder) and is equal to 3680 kN-m (2710 k-ft). D is determined based on a one-dimensional line girder analysis and equal to 672 kN-m (496 k-ft). Since no dynamic tests were carried out, I is calculated according to the *Standard Specifications for Highway Bridges*, as follows:

$$I = \frac{50}{L+125} \qquad (4)$$

where *L* is the span length of interest. With *L* equal to 25.6m (84ft), *I* is equal to 0.24. As a result, according to Eq. (3), the experimental and analytical $RF_{strength\_inventory}$ are equal to 2.49 and 1.12, respectively. The experimental and analytical estimations indicate that the Evanston Bridge is structurally adequate since both $RF_{strength\_inventory}$ are greater than 1.0. The former is expected to be higher than the latter since additional capacity not determined analytically was obtained through the field test.

3.2 *Ratio of Load Ratings*

To obtain the ratio of load ratings of the bridge at the positive moment location, the experimental $RF_{strength\_inventory}$ is divided by the analytical $RF_{strength\_inventory}$ and is equal to 2.22. The value indicates that the experimental load rating of the bridge is 2.22 times of the load rating calculated using the straight bridge grillage model. Note that the same value is obtained by taking the inverse ratio of live load effects (LL_A/LL_E) because the same R_n, D and I were assumed in both rating factors.

To obtain the effects of the different contributions for the ratio of load ratings, LL_E is first discretized and then divided by LL_A shown as follows:

$$\frac{LL_A}{LL_E} = \left(\frac{M_{LE}}{M_{total}}\right)\left(\frac{\sum STAT_{A,ST}}{\sum STAT_E}\right)\left(\frac{M_{total}}{M_{girder}+N\times a}\right)\left(\frac{M_{girder}+N\times a}{M_{girder}}\right)\left(\frac{DF_A\times m}{DF_E\times m}\right) \qquad (5)$$

where (M_{LE}/M_{total}) is the effect of the longitudinal distribution, ($\sum STAT_{A,ST}/\sum STAT_E$) is the effect of the additional stiffness in the system, ($M_{girder}+N\times a/M_{girder}$) is the effect of the unintended composite action, ($M_{total}/M_{girder}+N\times a$) is the effect of the slab flexure, and ($DF_A\times m/DF_E\times m$) is the effect of the lateral distribution. DF_A and DF_E are the analytical and experimental lateral distribution factors, respectively and are equal to 0.74 and 0.94, respectively. M_{LE} is the longitudinal adjustment moment and is equal to 613 kN-m (452 k-ft). The derivation and explanation of all the parameters and contributions are detailed in Lu (2020). The effect of each contribution is given in Table 1.

Table 1. Deaggregated ratio of load ratings at the positive moment location.

Contribution	Value
Longitudinal distribution	1.092
Additional stiffness	1.460
Slab flexure	1.010
Unintended composite action	1.752
Lateral distribution	0.787

For the longitudinal distribution, it was observed that approximately 9% less of the load is going to the maximum positive moment than what would be expected in the prismatic analysis. The additional stiffness introduced to the system is expected to be greater than 1.0 because this effect is not accounted in the theoretical model. However, the value seems to be over predicted since it provides an increase in capacity of approximately 50% in the experimental load rating compared to the analytical load rating. For the contribution of the slab flexure, since the slab and girder deflect with the same curvature with the latter much stiffer than the former, the contribution is expected to be small (1%). The effect of the actual lateral distribution reduced the load capacity by approximately 21% relative to the straight bridge grillage model. Although the contribution seems to be underpredicted, differences between DF_A and DF_E are expected since the analytical lateral distribution is only expressed in function of the transverse girder spacing while the actual lateral distribution also depends on the girder and edge stiffnesses (Catbas et al. 2012). The results showed that the unintended composite action has the dominant effect on the increase of the experimental load rating. However, this contribution may be unreliable because the friction resistance between the slab and the girder would be overcome for loads that exceed the elastic range (Lantshoght et al. 2017). Therefore, it is recommended to exclude this contribution when calculating the ratio of load ratings. Note that the product of all contributions is equal to the ratio of load ratings calculated without deaggregation (equal to 2.22). When removing the effect of unintended composite action by simply dividing the contribution out, the reliable load rating is equal to 1.27.

3.3 *Contribution of Skew Effect*

Based on the ratio of $\sum STAT_{A,ST}$ and $\sum STAT_{A,SK}$, the effect of additional stiffness introduced in the system due to the bridge skew is equal to 1.190. This contribution is expected to be greater than 1.0 because $\sum STAT_{A,ST}$ is always greater than $\sum STAT_{A,SK}$. Since the load path of the former is longer than the latter, a higher moment is obtained at the former as the moment calculation is directly proportional to the square of the span length.

Since the total additional stiffness introduced in the system is constant and to avoid double counting of the effect of additional stiffness due to the bridge skew, the former was divided by the latter so that the effect of additional stiffness due to curbs and railings is determined. Therefore, this contribution is equal to 1.227. A value greater than 1.0 is expected because, unlike in the actual behavior, the effect of railings was not considered in the grillage modeling. However, an increase of 23% of the experimental contribution over the analytical seems to be an over prediction. A reasonable value for this effect would be between 1% to 5%. The results would be further improved if the model were built with a more refined mesh and with a more accurate definition of the load positions, or if a finite element analysis of the bridge was conducted. Another factor that may have influenced the comparison of the additional stiffness and not considered in this study is the partial restraint of the supports. In fact, the experimental data strongly suggests this possibility since the equilibrium is not maintained in the moment diagram. If the restraint conditions were assumed at the abutment, the statical moment and consequently the additional stiffness introduced in the system would be modified.

3.4 *Partial Restraint of the Supports*

Unlike of what was expected, the effect of the additional stiffness due to curbs and railings seems to be too high and the effect of lateral distribution indicates that the analytical and actual distributions are considerably discrepant. Prior problems inherent to the modeling such as the crude assumptions made for the loading positions and for the stiffness of the curbs, it was found that the results obtained experimentally are not in statical equilibrium. The inconsistency was verified when the superimposed shear forces at the segments adjacent to the supports calculated due to the critical side-by-side truck loading do not add up to the weight of the three calibrated trucks. The shear forces can be obtained by taking the slopes that compose the experimental moment diagram since, according to principles of Mechanics of Materials, the rate of change of the bending moment, dM respective to the longitudinal span direction, x is equal to the shear force, V ($V=dM/dx$). To obtain the shear forces, the experimental moment diagram needs to be completed with the help of the moments determined at the location where the bridge was instrumented. The maximum positive moment, M_{max+}(1800 kN-m (1330 k-ft), corresponding to location D in Figure 8) occurs exactly when the middle axle of the truck is at a distance 0.4 times the span length measured from the abutment of the eastern span. For the moments at the front, M_{1+} and rear, M_{2+} axles (corresponding to locations E and C, respectively in Figure 8), since it is impossible to calculate them based on the strain-histories, the values were estimated by assuming to follow the same ratio between the moment at the middle axle and respective rear and front axles obtained using a one-dimensional line girder model. The values of M_{1+} and M_{2+} were obtained by multiplying M_{max+} to 0.722 and 0.971, respectively and are equal to 1300kN-m (957 k-ft) and 1750 kN-m (1290 k-ft), respectively. The negative moment at the instrumented location,M_{8ft-} is equal to -575 kN-m (-424 k-ft) which corresponds to location B in Figure 8. With the moment at the different points defined as well as the positions of the axle loads, the slope of the segments next to the eastern (location F in Figure 8) and western supports are calculated and illustrated as k_1 (215 kN-m/m (48.3 k-ft/ft)) and k_2 (200kN-m/m (44.9 k-ft/ft)), respectively in Figure 8. Note that the negative moment at the pier, M_{pier-} (-1060 kN-m (-783 k-ft), corresponding to location A in Figure 8) is calculated based on k_2 and M_{8ft-}. The remaining slopes were not calculated because they do not participate in the comparison to the applied load. In fact, the values would not match with the applied load since the moments at the rear and front axles were estimated based on the one-dimensional line girder analysis. The inconsistency was confirmed since the summation of k_1 and k_2 is 415 kN (93.2 k) which is relatively smaller than the summation of the load of the three trucks that represent the critical side-by-side truck loading,W_{3TRK}(609 kN (137 k)).
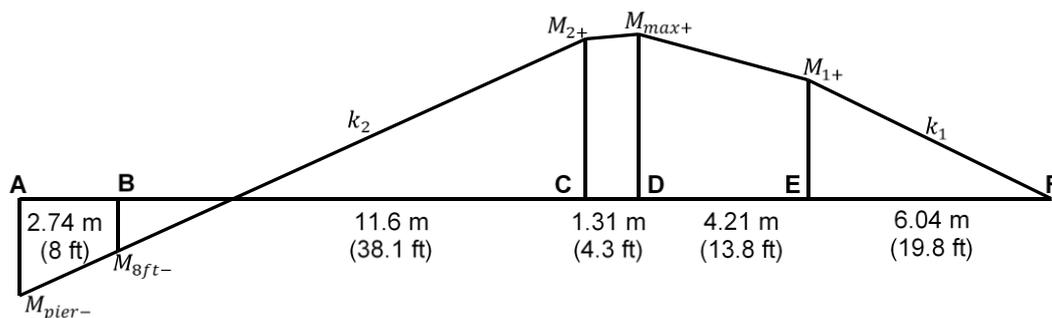
Figure 8. Experimental moment diagram of the outer eastern span.

The difference between the shear forces and W_{3TRK} suggests that some moment is resisted by the bearings even though they were designed as rollers. Accumulation of dust and temperature variation may add friction to the supports which cause them to freeze as a result (Algohi et al. 2019). To maintain the statical equilibrium of the system, the negative moment absorbed by the abutment, $M_{abutment-}$ is obtained, as follows:

$$M_{abutment \ -} = (W_{3TRK} - k_2) \times [EF] - M_{1+} \qquad (6)$$

where (EF) is the distance between the abutment to the front axle load illustrated in Figure 8. A value of -1170 kN-m (-866 k-ft) is obtained for the experimental $M_{abutment-}$. Based on the experimental $M_{abutment-}$ and M_{pier-}, the experimental statical moment is now equal to 2930 kN-m (2160 k-ft). Considering that the proportion is the same between $M_{abutment-}$ and M_{pier-} for both experimental and analytical results, since the analytical M_{pier-} is equal to -885 kN-m (-653 k-ft), the analytical $M_{abutment-}$ that would be at the abutment of the straight bridge grillage model is assumed to be -979 kN-m (-722 k-ft). As a result, the statical moment is equal to 3820 kN-m (2820 k-ft).

With the consideration of $M_{abutment-}$, the ratio between the analytical and experimental statical moments (additional stiffness introduced in the system) is now equal to 1.305. With the contribution of the bridge skew constant, the effect of additional stiffness due to the contribution curbs and railings is equal to 1.098. Although the contribution still seems to be a little high, the value is now closer to the limits of acceptance range. A more realistic way to determine the actual resisting moment is to determine the actual response by instrumenting the abutments. The proper method to account for the bearing restraints is to place a strain gage at the girder bottom flange located by the support and obtain the corresponding force based on its geometry. More details of this method can be found in Barker (2001).

4 CONCLUSIONS

In this study, the ratio of load ratings at the positive moment for a skewed four-span concrete slab on steel girders Highway Bridge was determined based on the results obtained in an experimental field test and using a straight bridge grillage modeling. For the bridge examined, the critical side-by-side truck loading occurs in Runs 3, 8, and 13 and the critical girder is Girder 3. The results showed a 27% increase in the experimental load rating over the analytical load rating even when the effect of unintended composite action between the slab and girders is removed. The contribution of additional stiffness to the load rating was discretized into two parts: the effect due to the bridge skew, and the effect due to curbs and railings. The effect due to bridge skew was obtained by comparing the statical moments determined using a non-skewed (straight) bridge grillage model and a skewed bridge grillage model. The results indicated that the angle of skew increases the bridge experimental load rating by 19%, relative to the load rating calculated for the equivalent straight bridge model. Due to the partial restraint of the abutments, the contribution of additional stiffness due to curbs and railings was overestimated. To better determine the contribution, field instrumentation at the bearing locations is necessary. Nevertheless, despite the need of additional testing to obtain improved results of the additional due to curbs and railings, the study demonstrates that the field test load rating procedure coupled with grillage modeling is a promising method to determine the actual behavior of skewed highway bridges.

The proposed procedure provides insight into the primary contributions to load rating and allows unreliable effects to be identified. Unlike a one-dimensional line girder model, the grillage modeling approach makes it possible to predict the effect of bridge skew. By determining the actual behavior of highway bridges, rather than following conservative requirements, more efficient measures of maintenance, posting and rehabilitation can be employed. The approach can also be used in continuous long-term monitoring studies. In addition, the findings of this research can also be used to calibrate analytical models for parametric studies.

REFERENCES

AASHTO (American Association of State Highway and Transportation Officials). 1996. *Standard specifications for highway bridges, 16th edition*. Washington, DC.
AASHTO (American Association of State Highway and Transportation Officials). 2011. *The manual for bridge evaluation, 2nd edition*. Washington, DC.
AASHTO (American Association of State Highway and Transportation Officials). 1996. *LRFD bridge design specifications*, *7th edition*. Washington, DC.
Algohi, B., Mufti, A., Bakht, B., Thomson, D. & Svecova, D. 2019. Monitoring of the variation of neutral axis in slab-on-girder bridge. *9th International Conference on Structural Health Monitoring of Intelligent Infrastructure*, 4-7August2019. St. Louis, Missouri, United States of America.
Badwin, I. Z. & Liang, R. Y. 2007. Reaction and distribution in highly skewed continuous steel girder bridge testing and analysis. *Transportation Research Record* 2028(1): 163-170.

Barker, M. G. 1999. Steel girder bridge field test procedures. *Construction and Building Materials.*13(4): 229-239.

Barker, M. G. 2001. Quantifying field-test behavior for rating steel girder bridges. *Journal of Bridge Engineering* 6(4): 254-261.

BDI (Bridge Diagnostics Inc.). 2015. *ST350 Operations Manual*. Louisville, Colorado, United States of America.

Cai, C. S. &Shahawy, M. 2003. Understanding capacity rating of bridges from load tests. *Practice Periodical on Structural Design and Construction* 8(4): 209-216.

Catbas, F. N., Gokce, H. B. & Gul, M. 2012. Practical approach for estimating distribution factor for load rating: demonstration on reinforced concrete T-beam bridges. *Journal of Bridge Engineering* 14(4): 652-661.

Chajes, M. J., Shenton, H. W. & O'Shea, D. 2000. Bridge-condition assessment and load rating using nondestructive evaluation methods. *Journal of the Transportation Research Board* 1696(1): 83-91.

Huang, H., Shenton, H. W. & Chajes, M. J. 2004. Load distribution for a highly skewed bridge: testing and analysis. *Journal of Bridge Engineering* 9(6): 558-562.

Jáuregui, D. V. & Barr, P. J. 2004. Nondestructive evaluation of the I-40 bridge over the Rio Grande river. *Journal of Performance of Constructed Facilities* 18(4): 195-204.

Lantsoght, E. O. L., van der Veen, C. and de Boer, A. & Hordijk, D. A. 2017. State-of-the-art of load testing of concrete bridges. *Engineering Structures*150(1): 231-241.

Lu, R. 2020. Experimental Load Rating of Skewed Steel Girder Highway Bridges. PhD thesis. University of Wyoming, Laramie, Wyoming.

Sanayei, M., Reiff, A. J., Brenner, B. R. &Imbaro, G. R. 2016. Load rating of a fully instrumented bridge: comparison of LRFR approaches. *Journal of Performance of Constructed Facilities* 30(2): 04015019.

Yarnold, M., Golecki, T. & Weidner, J.2018. Identification of composite action through truck load testing. *Frontiers in Built Environment* 4(74): 1-13.